

# A lattice model of reduced jamming by barrier

Emilio N.M. Cirillo,<sup>1,\*</sup> Oleh Krehel,<sup>2,†</sup> Adrian Muntean,<sup>3,‡</sup> and Rutger van Santen<sup>4,§</sup>

<sup>1</sup>*Dipartimento di Scienze di Base e Applicate per l'Ingegneria,  
Sapienza Università di Roma, via A. Scarpa 16, I-00161, Roma, Italy.*

<sup>2</sup>*ICMS – Institute of Complex Molecular Systems,  
Department of Mathematics and Computer Science, Eindhoven University of Technology,  
P.O. Box 513, 5600 MB Eindhoven, The Netherlands.*

<sup>3</sup>*Department of Mathematics and Computer Science, Karlstad University, Sweden.*

<sup>4</sup>*ICMS – Institute for Complex Molecular Systems,  
Faculty of Chemical Engineering, Eindhoven University of Technology,  
P.O. Box 513, 5600 MB Eindhoven, The Netherlands,*

We study an asymmetric simple exclusion process in a strip in the presence of a solid impenetrable barrier. We focus on the effect of the barrier on the residence time of the particles, namely, the typical time needed by the particles to cross the whole strip. We explore the conditions for reduced jamming when varying the environment (different drifts, reservoir densities, horizontal diffusion walks, etc.). Particularly, we discover an interesting non-monotonic behavior of the residence time as a function of the barrier length. Besides recovering by means of both the lattice dynamics and mean-field model well-known aspects like faster-is-slower effect and the intermittence of the flow, we propose also a birth-and-death process and a reduced one-dimensional model with variable barrier permeability to capture qualitatively the behavior of the residence time with respect to the parameters. We report our first steps towards the understanding to which extent the presence of obstacles can fluidize pedestrian and biological transport in crowded heterogeneous environments.

PACS numbers: 05.40.Fb; 02.70.Uu; 64.60.ah

## I. INTRODUCTION

Lattice models of particle flow may show surprisingly rich behavior even when only exclusion of a particle on the same site is considered [1]. Complex percolation behavior arises in particular at increased particle concentration (see [2] for a modern account on percolation theory, [3] for a case study related to the motion of colloids in narrow channels, and [4] for percolation effects in transportation in more general complex systems). In this paper, we introduce a two dimensional asymmetric simple exclusion random walk model with diffusion and drift. The model aims at capturing the effect of the barrier positioned in the strip on the corresponding residence times, i.e., the time needed by a particle to cross the strip.

More precisely, we consider a (say) vertical strip and measure the time that a particle entering the strip at the top side takes to exit the strip through the bottom side, under the assumption that the three other boundaries act

as reflecting boundaries. This typical time will be called *residence time*.

We find an interesting non-linear dependence on the length of this barrier when simulating the evolution of a high particle density in the strip. Instead of the expected increase in the residence time, at particular conditions we surprisingly notice a decrease in residence times with increasing barrier length. This reminds us of the Braess paradox, discovered when traffic flow unexpectedly decreases, whereas an inhibitive traffic access barrier is removed (cf. [5]). This confirms once more the fact that as population densities and the number of interactions between particles (agents, people, financial stocks, etc.) increase, so does the probability of emergent phenomena.

Our modeling approach and simulation results are potentially useful when trying to forecast the motion of pedestrian flows in open (heterogeneous) spaces. It has for instance been found that flocking of sheep [6, 7] is helped by introducing a barrier before an exit point. Also high density particle flow through an orifice that leads to jamming has been found to have less jamming when a barrier is put in front of the orifice (see, for instance, [8] and [9] for crowd dynamics scenarios when the flow is improved by the presence of an obstacle in front of the

\* emilio.cirillo@uniroma1.it

† o.krehel@tue.nl

‡ adrian.muntean@kau.se

§ R.A.v.Santen@tue.nl

exit).

We have explored extensively in a previous paper (see [1]) the two dimensional diffusion–drift strip lattice model used in this context, but without barriers. On the two dimensional lattice a discrete stochastic process is simulated controlled by top and bottom reservoir densities. The displacement probabilities of the particles are in four directions:  $h$ ,  $u$ ,  $d$ , with  $h + u + d = 1$ . Displacements only can occur to a square lattice site that is unoccupied. The horizontal displacement probability perpendicular to the flow direction of the strip is  $h/2$ , whereas  $u$  and  $d$  are the upward and downward displacement probabilities. The model describes diffusion as well nonlinear convection when  $d - u$  is different from zero.

When the drift (pointing out in the top-down direction) is non-zero, our stochastic simulations show a phase transition in the dependence of simulated average particle residence time as a function of the barrier length  $W$ . This phase transition is only found when the density  $\rho_d$ , i.e., the bottom reservoir density, exceeds a particular value, while the range of barrier lengths of decreases in residence time depends on the choice of the drift value. In the absence of the drift, alike phase transitions do not happen (as predicted for instance in [10] and references cited therein).

Denote our vertical strip by  $\Omega$  and refer to the internal obstacle as  $\mathcal{O}$ , see Figure 2.2 for a sketch of the geometry. The physical basis of this phenomenon can be understood based on the particle density profiles. The calculated density profiles around the phase transition are shown for a particular situation in Figure 1.1 (the meaning of the parameters listed in the caption will be explained in Section II). One notes the transformation of a convex-to-concave density profile behind the barrier when the barrier width is moved through the phase transition regime. This density profile can be well approximated as solution to the mean-field equation

$$\frac{\partial \rho}{\partial t} = \frac{h}{2} \frac{\partial^2 \rho}{\partial y^2} + \frac{1-h}{2} \frac{\partial^2 \rho}{\partial x^2} - \delta(1-h) \frac{\partial}{\partial x} (\rho(1-\rho)) \quad (1.1)$$

in  $\Omega \setminus \mathcal{O}$ , endowed with the initial condition

$$\rho(0, y, x) = 0 \text{ in } \Omega \setminus \mathcal{O} \quad (1.2)$$

and the boundary conditions

$$\rho(t, y, 0) = \rho_u, \quad \rho(t, y, L_2) = \rho_d, \quad (1.3)$$

and

$$\frac{\partial \rho(t, 0, x)}{\partial y} = \frac{\partial \rho(t, L_1, x)}{\partial y} = \nabla \rho \cdot n_{\partial \mathcal{O}} = 0. \quad (1.4)$$

Here  $n_{\partial \mathcal{O}}$  denotes the outer normal along the boundary of the obstacle  $\mathcal{O}$ .

It occurs to us that there may not be too much dependence in the density profile on the  $y$  variable and we can approximate the two dimensional density profile with its one dimensional counterpart  $\tilde{\rho}(x)$  that we obtain by integrating out the  $y$  variable. This one dimensional density profile can be then used to calculate the residence time estimate that is given from the mean field expression

$$R = -\frac{2}{(1-h)\partial_x \tilde{\rho}(0)} \int_0^{L_2} \tilde{\rho}(x) dx. \quad (1.5)$$

This expression [1, equation (5.35)] shows that the average particle residence time is determined by the derivative of the density at the entrance of the strip and the integrated density. The convex to concave density profile change behind the barrier in Figure 1.1 indicates a large change in the particle density, that, as we will see, is responsible to a significant extend to the phase transition behavior. We have discussed previously in [1] that the mean field equation (1.1) is only valid in a limited regime of the parameter space, there a birth-and-death random walk model providing an alternative approach to calculate the residence time is proposed.

Non-linear behaviors in the residence time are not limited to the dependence on the barrier width (that occurs when the drift is not zero). Parametric dependencies can turn to be non-monotonic as well. It is worth noting that in absence of drift, the dependence on the barrier width always turns into a monotonic decrease of the residence time with increasing width. However, mind that this decrease does not uniformly scale with the lateral strip dimension. When the residence times are considered at similar ratios of barrier width and strip lateral dimension, the corresponding residence times are found to increase with increasing the strip lateral dimension. The effect depends on the horizontal hopping probability and diminishes when the hopping frequency becomes larger.

In addition to the numerical solution of the residence time on the one dimensional density profiles determined by averaging the density of the two dimensional simulations, approximate analytical solutions are sought for the corresponding viscous one-dimensional Burgers equation, which has then to be solved together with the proper boundary conditions.

The paper is organized as follows. In Section II, we introduce the lattice model and the different methods to approach the barrier problem. This is to be followed by

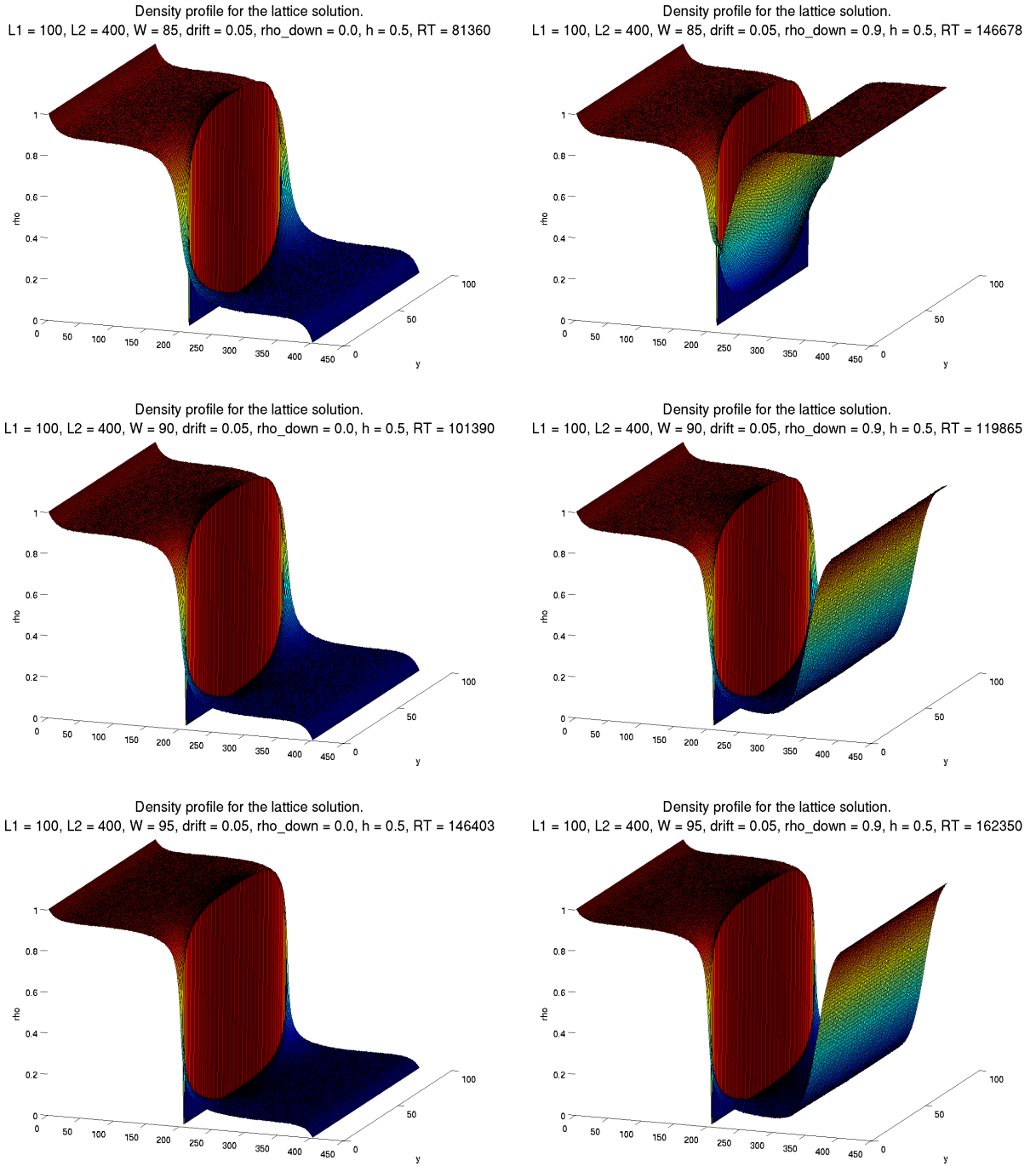


FIG. 1.1. 2D density profiles. On the left,  $\rho_d = 0.0$  and the average residence times are 81359.8, 101390, 146403. On the right,  $\rho_d = 0.9$  and the average residence times are 146678, 119865, 162350. The other parameters are  $L_1 = 100$ ,  $L_2 = 400$ ,  $h = 0.5$ ,  $\delta = 0.05$ ,  $\rho_u = 1$ ,  $O_2 = 3$ , and  $W = 85$  (top),  $W = 90$  (middle),  $W = 95$  (bottom).

the presentation of our results in Section III and IV. Essentially, we compare the two dimensional model simulations with the output of the 1D model and give evidence of the occurrence of a phase transition in one dimension. The paper is concluded with a short discussion of the

results in Section V.

## II. MODELS AND METHODS

In this section, we introduce the models we plan to study to address the problem discussed in the introduction and we shall also give a brief account of our main methods.

### A. Lattice dynamics

The lattice model we discuss in this paper is the same as the one introduced in [1], excepting for the presence of the obstacle. Nevertheless, for the sake of clarity we define the model in detail.

Take  $L_1, L_2 \in \mathbb{N}$ . Let  $\Lambda \subset \mathbb{Z}^2$  denote the *strip*  $\{1, \dots, L_1\} \times \{1, \dots, L_2\}$ . We say that the coordinate directions 1 and 2 of the strip are respectively the *horizontal* and the *vertical* direction. We accordingly use the words *top*, *bottom*, *left*, and *right*. On  $\Lambda$  we define a discrete time stochastic process controlled by the parameters  $\varrho_u, \varrho_d \in [0, 1]$  and  $h, u, d \in [0, 1]$  such that  $h + u + d = 1$ . The meaning of the parameters is clarified in what follows.

The *configuration* of the system at time  $t \in \mathbb{Z}_+$  is given by the positive integer  $n(t)$  denoting the number of particles in the system at time  $t$  and by the two collections of integers  $x_1(1, t), \dots, x_1(n(t), t) \in \{1, \dots, L_1\}$  and  $x_2(1, t), \dots, x_2(n(t), t) \in \{1, \dots, L_2\}$  denoting, respectively, the horizontal and the vertical coordinates of the  $n(t)$  particles in the strip  $\Lambda$  at time  $t$ . The  $i$ -th particle, with  $i = 1, \dots, n(t)$ , is then associated with the site  $(x_1(i, t), x_2(i, t)) \in \Lambda$  which is called *position* of the particle at time  $t$ . A site associated with a particle a time  $t$  will be said to be *occupied* at time  $t$ , otherwise we shall say that it is *free* or *empty* at time  $t$ . Fix  $n(0) = 0$ .

At each time  $t \geq 1$  we first set  $n(t) = n(t-1)$  and then repeat the following algorithm  $n(t-1)$  times. Essentially, at each step of the dynamics, a number of particles equal to the number of particles in the system at the end of the preceding time  $n(t-1)$  is tentatively moved. One of the three actions *insert a particle through the top boundary*, *insert a particle through the bottom boundary*, and *move a particle in the bulk* is performed with the corresponding probabilities  $\varrho_u L_1 / (\varrho_u L_1 + \varrho_d L_1 + n(t))$ ,  $\varrho_d L_1 / (\varrho_u L_1 + \varrho_d L_1 + n(t))$ , and  $n(t) / (\varrho_u L_1 + \varrho_d L_1 + n(t))$ .

*Insert a particle through the top boundary.* Chose at random with uniform probability the integer  $i \in \{1, \dots, L_1\}$  and, if the site  $(1, i)$  is empty, with probability  $d$  set  $n(t) = n(t) + 1$  and add a particle to site

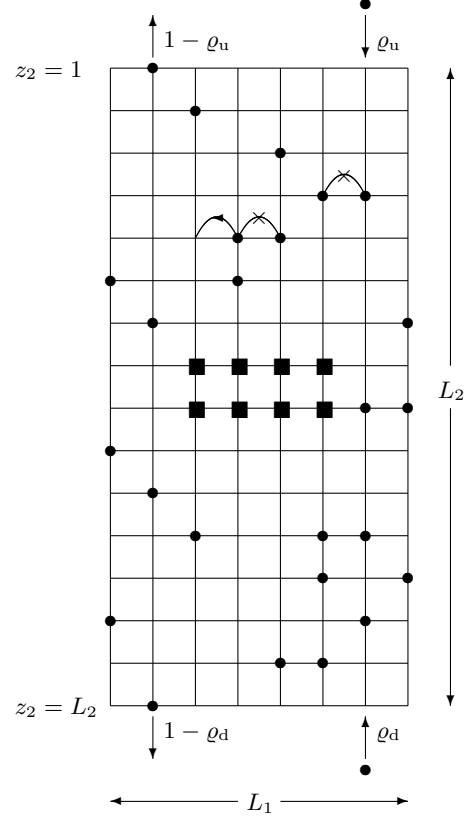


FIG. 2.2. Schematic representation of the model in the presence of the barrier. Solid squares represent the particles at rest modeling the obstacle.

$(1, i)$ .

*Insert a particle through the bottom boundary.* Chose at random with uniform probability the integer  $i \in \{1, \dots, L_1\}$  and, if the site  $(L_2, i)$  is empty, with probability  $u$  set  $n(t) = n(t) + 1$  and add a particle to site  $(L_2, i)$ .

*Move a particle in the bulk.* Chose at random with uniform probability one of the  $n(t)$  particles in the bulk. The chosen particle is moved according to the following rule: one of the four neighboring sites of the one occupied by the particle is chosen at random with probability  $h/2$  (left),  $u$  (up),  $h/2$  (right), and  $d$  (down). If the chosen site is in the strip (not on the boundary) and it is free, the particle is moved there leaving empty the site occupied at time  $t$ . If the chosen site is on the boundary of the strip the dynamics is defined as follows: the left boundary  $\{(0, z_2), z_2 = 1, \dots, L_2\}$  and the right boundary  $\{(L_1 + 1, z_2), z_2 = 1, \dots, L_2\}$  are *reflecting* (homogeneous Neumann boundary conditions) in the sense that a particle trying to jump there is not moved. The bottom

and the top boundary conditions are stochastic in the sense that when a particle tries to jump to a site  $(z_1, 0)$ , with  $z_1 = 1, \dots, L_1$ , such a site has to be considered occupied with probability  $\varrho_u$  and free with probability  $1 - \varrho_u$ , whereas when a particle tries to jump to a site  $(z_1, L_2 + 1)$ , with  $z_1 = 1, \dots, L_1$ , such a site has to be considered occupied with probability  $\varrho_d$  and free with probability  $1 - \varrho_d$ . If the arrival site is considered free the particle trying to jump there is removed by the strip  $\Lambda$  (it is said to *exit* the system) and the number of particles is reduced by one, namely,  $n(t) = n(t) - 1$ . If the arrival site is occupied the particle is not moved.

*Particle meets barrier.* The impenetrable barrier is modeled by a rectangular region of width  $W$  and height  $O_2$  which is constantly occupied by particles at rest. Hence, particles moving on the lattice must do back step and/or lateral jump this region.

It is worth noting that the model is a Markov chain  $\omega_0, \omega_1, \dots, \omega_t, \dots$  on the *state* or *configuration space*  $\Omega := \{0, 1\}^\Lambda$  with transition probability that can be deduced by the algorithmic definition.

This model will be studied via Monte Carlo simulations. We will let evolve the process for a time (*thermalization time*) sufficiently long until the system reach the state. After that, we shall measure the two-dimensional density profile by averaging the occupation number at each site of the lattice (see, for instance, Figure 1.1).

Moreover, we shall also measure the residence time by averaging, at stationarity, the time needed by a particle entered through the top boundary to exit through the bottom one. In this computation the top boundary condition will be chosen to be  $\rho_u = 1$  so that particles will not be allowed to leave the system through the top boundary.

In the study of the residence time we shall find two very different pictures in the case in which the dynamics will be either biased or not along the vertical direction. A special role, hence, will be played by the parameter

$$\delta = \frac{d - u}{d + u} \quad (2.6)$$

which will be called *drift*.

For more details we refer the reader to [1] where a complete account on these techniques has been provided.

## B. Mean field dynamics

The mean field equation (1.1) corresponds to the lattice dynamics presented in Subsection II A. It is derived

in full details in [1], using arguments very much inspired from [11]. We refer the reader to these papers for the details of the derivation of the mean field model and particularly to [1] for a detailed investigation of its validity range depending on the relative sizes of the most influential model parameters. The novelty here is the presence of the obstacle. The derivations follow similarly under the assumption that the obstacle is impenetrable.

This mean field model is studied via a finite element approach. The problem (1.1)–(1.4) is integrated numerically and the density profile  $\rho(y, x)$  is found. Then the residence time is computed by means of the equation (1.5).

We used the Finite Element Numerics toolbox DUNE [18] to implement a solver for the model. We used quadratic Lagrange elements and the Newton method to deal with the nonlinear drift term.

## C. One-dimensional reduction

We propose a twofold reduction of the Mean Field model. This way, we reduce the dimensionality of the model from 2D to 1D and compensate, based on an effective transport coefficient, for the presence of the obstacle. For this we use a porous media modeling approach where parameters like obstacle porosity and tortuosity will be used in the 1D context. Similar arguments are indicated, for instance, in [12].

It occurs to us that there may be not too much dependence in the density profile on the  $y$  variable and we can approximate the two dimensional density profile with its one dimensional counterpart that we obtain by integrating out the  $y$  variable. After integration, the  $x$  coordinates that correspond to the place where the obstacle was in two dimensions, are designated to have a smaller diffusion coefficient to account for that obstacle.

In our initial approximation, we consider the diffusion coefficient and the drift to be porosity and tortuosity based via the coefficient

$$\lambda(x) = \begin{cases} F(h) \frac{L_1 - W}{L_1} & x \in [\frac{L_2 - O_2}{2}, \frac{L_2 + O_2}{2}] \\ 1 & \text{otherwise.} \end{cases} \quad (2.7)$$

For convenience we also let  $\alpha := F(h)(L_1 - W)/L_1$ . Here, the ratio  $(L_1 - W)/L_1$  is the porosity, while  $F(h)$  is the currently unknown function of the horizontal displacement probability  $h$ . This plays the role of the tortuosity. It is expected that  $F(h) \in (0, 1)$ . In this very basic

approximation porosity and tortuosity effects are independent (multiplicative), so that the no obstacle case is recovered for  $W = 0$  and  $F(h) = 1$  in the expression (2.7). An increase in  $W$  results in a decrease in  $\lambda(x)$  in the region  $x \in [(L_2 - O_2)/2, (L_2 + O_2)/2]$ , which is also the expected behavior from the lattice model.

The 1D Mean Field equation reads

$$\frac{d}{dx} \left[ \lambda(x) \left( \frac{1}{2} \frac{d\rho}{dx} - \delta \frac{d}{dx} (\rho(1 - \rho)) \right) \right] = 0 \quad (2.8)$$

with the boundary conditions

$$\rho(0) = 1 \quad \text{and} \quad \rho(L_2) = \rho_d. \quad (2.9)$$

On the basis of the density profile obtained by solving (2.8), it is possible to compute the residence time via a standard argument, see, e.g., [1, Section 5.6]. We find

$$R = -\frac{2}{\rho'(0)} \int_0^{L_2} \rho(x), \quad (2.10)$$

which is the analogous of equation (1.5).

We will see in the next Section that the reduced model (2.8) and (2.9) is a convenient approximation of the 2D mean-field model with obstacle in the zero drift case. In this context the model will be solved explicitly and the density profile will be computed. Then we will compute the residence time using again (1.5).

### III. ZERO DRIFT CASE

We consider the lattice model introduced in Section II A on the lattice strip of size  $L_1 \times L_2$  in absence of drift, namely, for  $\delta = 0$ . Our simulations will be run mainly for  $L_1 = 100$ ,  $L_2 = 400$ ,  $h = 0.5$ ,  $\rho_u = 1$ , and  $\rho_d = 0, 0.9$ . But in some cases we shall also consider the values  $L_1 = 200$  and  $h = 0.3, 0.4$ . Our obstacle is of size  $W \times O_2$  and is placed in the middle of the strip. The typical values used in the simulations for the width  $W$  of the obstacle are 10, 20, ..., 90. Its height  $O_2$  will always be equal to 3.

In this case, since particles do not experience any external drift, we expect that the stationary density profile will poorly depend on the horizontal lattice coordinate. For this reasons it appears reasonable to compare our Monte Carlo results for the lattice model with estimates based on the one dimensional model introduced in Section II C.

#### A. Solution to the 1D model

For  $\delta = 0$  the model in Section II C simplifies and a thorough analytical treatment is possible. The 1D equation (2.8) is a linear diffusion equation with a piecewise constant diffusion coefficient. Its solution is piecewise linear on intervals  $[0, (L_2 - O_2)/2]$ ,  $[(L_2 - O_2)/2, (L_2 + O_2)/2]$ ,  $[(L_2 + O_2)/2, L_2]$ , and we can express it in the form

$$\rho(x) = \rho_u T_0(x) + a T_1(x) + b T_2(x) + \rho_d T_3(x), \quad (3.11)$$

where the coefficients  $a$  and  $b$  are the unknowns. The functions  $T_i$  are the linear pyramid functions. Their derivatives are  $T'_0(x) = -2/(L_2 - O_2)$  on  $[0, (L_2 - O_2)/2]$  and 0 otherwise,

$$T'_1(x) = \begin{cases} \frac{2}{L_2 - O_2} & \text{on } [0, (L_2 - O_2)/2], \\ -\frac{1}{O_2} & \text{on } [(L_2 - O_2)/2, (L_2 + O_2)/2], \\ 0 & \text{otherwise} \end{cases}$$

$$T'_2(x) = \begin{cases} \frac{1}{O_2} & \text{on } [(L_2 - O_2)/2, (L_2 + O_2)/2], \\ -\frac{2}{L_2 - O_2} & \text{on } [(L_2 + O_2)/2, L_2], \\ 0 & \text{otherwise.} \end{cases}$$

and  $T'_3(x) = 2/(L_2 - O_2)$  on  $[(L_2 + O_2)/2, L_2]$  and 0 otherwise. After substituting (3.11) into (2.8), multiply both sides by  $T_1(x)$  and  $T_2(x)$  and then integrate. This yields the following equations

$$\int_0^{L_2} \rho'(x) D(x) T'_1(x) = 0 \quad \text{and} \quad \int_0^{L_2} \rho'(x) D(x) T'_2(x) = 0.$$

From here it follows that

$$\int_0^{\frac{L_2 - O_2}{2}} (\rho_u T'_0 + a T'_1) T'_1 + \int_{\frac{L_2 - O_2}{2}}^{\frac{L_2 + O_2}{2}} (a T'_1 + b T'_2) \alpha T'_1 = 0$$

and

$$\int_{\frac{L_2 - O_2}{2}}^{\frac{L_2 + O_2}{2}} (a T'_1 + b T'_2) \alpha T'_2 + \int_{\frac{L_2 + O_2}{2}}^{L_2} (b T'_2 + \rho_d T'_3) T'_2 = 0.$$

After integration, we obtain the next linear system

$$\begin{aligned} \frac{1}{L_2 - O_2} (a - \rho_u) + \frac{\alpha}{O_2} (b - a) &= 0, \\ \frac{\alpha}{O_2} (b - a) - \frac{1}{L_2 - O_2} (\rho_d - b) &= 0. \end{aligned}$$

yielding

$$a = \frac{\rho_u + \rho_d + \rho_u \beta}{2 + \beta} \quad \text{and} \quad b = \frac{\rho_u + \rho_d + \rho_d \beta}{2 + \beta}, \quad (3.12)$$

with

$$\beta = \frac{O_2}{\alpha(L_2 - O_2)}. \quad (3.13)$$

We remark that the deviations in the density profile from the straight line are symmetric. See e.g. Figure 3.4 for an example simulation. Indeed, by summing the coefficients in (3.12) we obtain  $a + b = \rho_u + \rho_d$  and, hence,

$$a - \frac{\rho_u + \rho_d}{2} = \frac{(\rho_u - \rho_d)\beta}{4 + 2\beta}$$

and

$$\frac{\rho_u + \rho_d}{2} - b = \frac{(\rho_u - \rho_d)\beta}{4 + 2\beta}.$$

Having obtained the analytical expression for  $\rho(x)$ , we can compute the 1D Mean Field residence time approximation by using (2.10). Indeed, some simple algebra yields

$$R = \frac{(\rho_u + \rho_d)L_2(L_2 - O_2)(2 + \frac{2O_2}{\alpha(L_2 - O_2)})}{\rho_u - \rho_d} \quad (3.14)$$

where, we recall,  $\alpha = F(h)(L_1 - W)/L_1$ . In the case  $\alpha = 1$ , i.e., no obstacle, the expression of the residence time simplifies to

$$R = \frac{(\rho_u + \rho_d)2L_2^2}{\rho_u - \rho_d}, \quad (3.15)$$

which is an agreement with [1, equation (5.39)].

We note the following: according to (3.14), the residence time increases with increasing value of  $\rho_d$ . Additionally, the effect of  $W$  on the residence time disappears when  $L_2$  goes to infinity. Moreover, from (3.14), the residence time uniformly increases as  $W$  increases. Note also that the  $W$  dependence can be also seen purely as  $W/L_1$ . This is a limitation of our simple approximation to the diffusion coefficient, since in our simulations we see an effect of different values of  $W$  on the residence time, even with the same  $W/L_1$  ratio (see Section III C).

### B. Density profile

Now, we discuss how the density profile obtained from (3.11) compares to the one obtained by averaging the 2D Monte Carlo simulation. The results are shown in Figure 3.3 in the case  $W = 70$ . The parameters we used in the computation are listed in the caption.

The match between the Monte Carlo and the analytical result is perfect. For the 1D model we had to optimize on

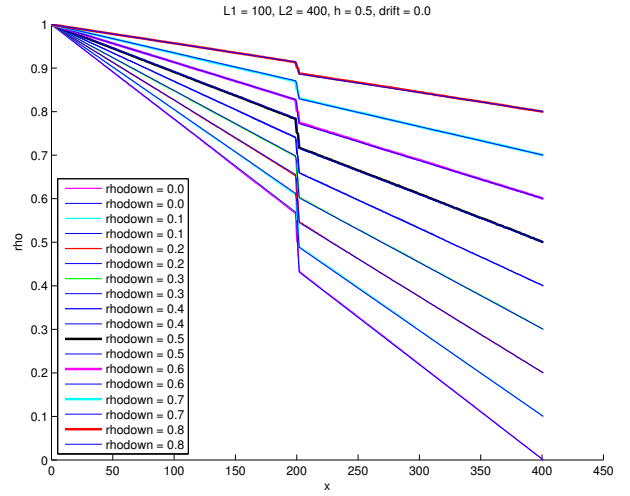


FIG. 3.3. Comparison between the density profile obtained by averaging the 2D lattice simulation and the analytical solution of the 1D mean field equation. Parameters:  $L_1 = 100$ ,  $L_2 = 400$ ,  $h = 0.5$ ,  $\delta = 0$ ,  $W = 70$ ,  $O_2 = 3$ ,  $\rho_u = 1$ , and  $\rho_d$  as listed in the inset. For the 1D model the tortuosity coefficient has been chosen equal to 0.45 for all the values of  $\rho_d$ . Thick lines correspond to Monte Carlo data for the lattice model and thin lines correspond to the analytical solution of the 1D model.

the tortuosity coefficient by choosing  $F = 0.45$  for this comparison, but we stress that the same value has been used for all the choices of the bottom boundary density plotted in the picture. Although this value resulted in a good match, the question of the explicit dependence  $F(h)$  still remains open.

The size of the jump in the averaged density profile, which can be observed in the figure, obviously depends on the width of the obstacle. This dependence is analyzed in Figure 3.4, where we plot the averaged Monte Carlo density profile for the 2D lattice model for different values of  $W$ . The two plots show our results for  $\rho_d = 0$  (top panel) and  $\rho_d = 0.9$  (bottom panel). It is worth remarking that, as we expected, in both cases the size of the jump increases with the obstacle width. But we stress that the qualitative behavior of the graph does not change with  $\rho_d$ . This fact is particularly relevant and it is key in our explanation for the different behaviors that we shall find in the biased (not zero drift) case.

### C. Residence time

The above discussion shows that the 2D stationary density profile can be found by averaging the Monte Carlo

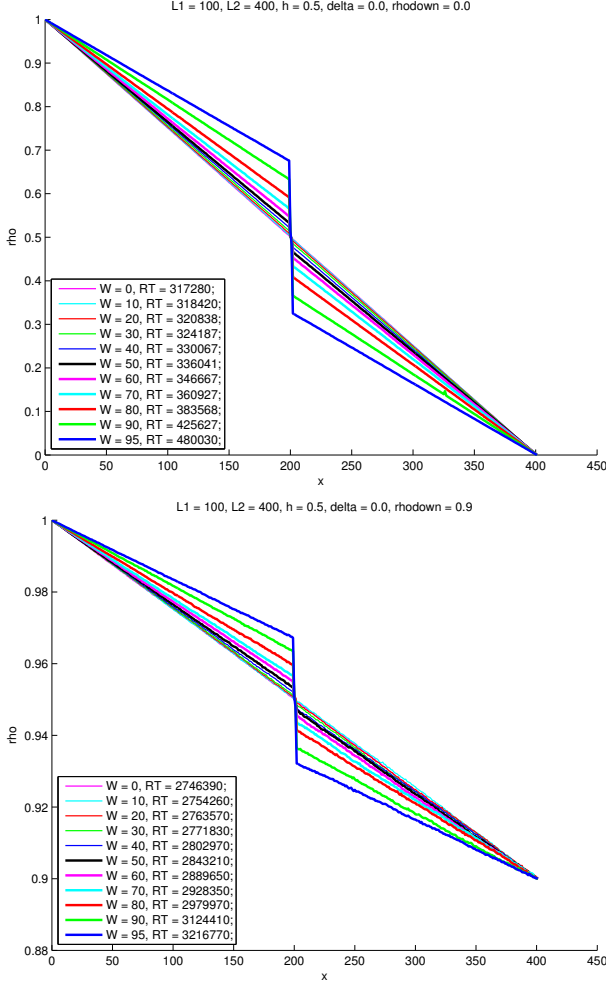


FIG. 3.4. Density profile obtained by averaging the 2D lattice simulation: comparison for different  $W$ . Parameters:  $L_1 = 100$ ,  $L_2 = 400$ ,  $h = 0.5$ ,  $\delta = 0$ ,  $\rho_u = 1$ ,  $\rho_d = 0$  (top) and  $\rho_d = 0.9$  (bottom),  $O_2 = 3$ , and  $W$  as listed in the inset. In the inset we have also listed the residence time data discussed in Section III C.

data for the 2D lattice model or by solving the Mean Field model (1.1). Moreover, by averaging along the horizontal axis this 2D profile, we find a 1D profile which can be perfectly fitted with the 1D model proposed in Section II C by choosing the correct tortuosity coefficient. Such a 1D density profile can be used as an input to estimate the residence time.

This estimate can be achieved via the Mean Field approximation provided in (1.5). In [1] a different approach, base on a Birth-and-Death model has been also proposed and thoroughly discussed in absence of obstacles. The main idea is that of predicting the residence time via a one-dimensional model in which a particle perform a simple random walk in the vertical direction with jumping

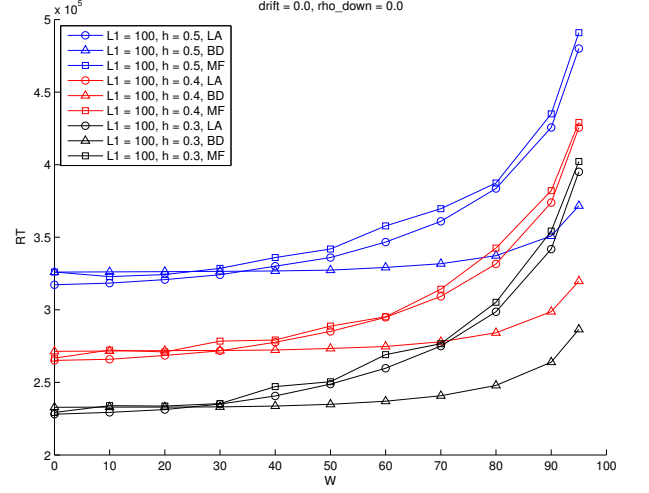


FIG. 3.5. The BD and MF approximations to the actual measured mean residence time (labeled LA). Parameters:  $L_1 = 100$ ,  $L_2 = 400$ ,  $\delta = 0$ ,  $\rho_u = 1$ ,  $\rho_d = 0$ ,  $O_2 = 3$ , and  $h$  as listed in the inset.

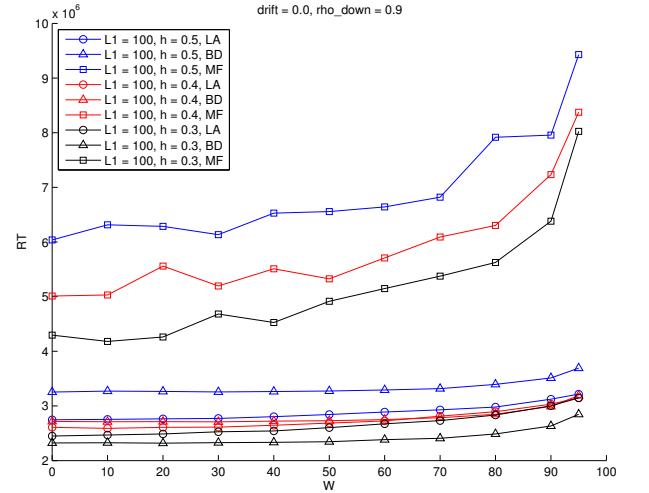


FIG. 3.6. The BD and MF approximations to the actual measured mean residence time (labeled LA). Parameters:  $L_1 = 100$ ,  $L_2 = 400$ ,  $\delta = 0$ ,  $\rho_u = 1$ ,  $\rho_d = 0.9$ ,  $O_2 = 3$ , and  $h$  as listed in the inset.

probabilities defined in terms of the stationary density profile measured for the 2D lattice model. In particular it has been deduced the prediction [1, equation (4.20)] for the residence time based on the Birth-and-Death model defined in [1, equation (5.28)]. In that paper, due to the absence of obstacle, the reduction to 1D is rather obvious, since the density profile does not depend on the horizontal coordinate. As already remarked above, in the present case we shall use this theory starting from the horizontally averaged density  $\bar{\rho}$  as in equation 1.5.



In Figure 3.5 and Figure 3.6, we compare the Monte Carlo measurement of the residence time to the Birth-and-Death and Mean Field estimates based on the horizontally averaged 1D density profile of a 2D simulation of a flow through a strip with an obstacle in the middle. On the horizontal axis we have the obstacle width and on the vertical axis the mean residence time. The formulas for the both residence time estimates can be found in [1], more precisely, see [1, equation (5.32)] and [1, equation (5.39)] respectively for the BD and the MF approximation.

As we can see, the quality of the approximation is influenced heavily by the value of  $\rho_d$ . For  $\rho_d = 0$ , the MF approximation works very well, while the BD approximation gets worse when the width of the obstacle is increased. For  $\rho_d = 0.9$ , the MF approximation overestimates by a lot, while the BD approximation is a bit better, but still not very precise. This result is consistent with what it has been found in [1] in absence of obstacle: in absence of drift, provided  $h$  is large enough (here we are using  $h = 0.5$ ), the BD prediction is better than the MF one in those situations in which clogging is present. There, in absence of obstacles, clogging was introduced by increasing the value of the bottom boundary density.

From this it follows that we can't expect to get great residence time estimates based on the analytical solution of our 1D model for the case of zero drift. But we can still hope to reproduce the density profiles well.

As a final remark, on which we shall come back in the discussion Section V in connection with the results we will find in the not zero drift situation, we note that the behavior of the residence time with the obstacle width is absolutely trivial. Indeed, it stays more or less constant till half the horizontal width is reached, then it increases sharply.

#### IV. NON-ZERO DRIFT CASE

We consider the lattice model introduced in Section II A on the lattice strip of size  $L_1 \times L_2$  in presence of drift, namely, for  $\delta > 0$ . Our simulations will be run mainly for the same parameters as those used in Section III. Details will be given in the figure captions.

In this case, since particles do experience an external drift, we expect that the stationary density profile will depend on the horizontal lattice coordinate. For this reasons our discussion will rely exclusively on the Monte Carlo simulation of the 2D lattice model introduced in

Section II A.

#### A. Density profile

The density profile is measured for the 2D lattice model, see also the comments Section II A, by averaging the occupation number at stationarity. Our results are plotted in Figure 1.1, where we used the parameters  $L_1 = 100$ ,  $L_2 = 400$ ,  $h = 0.5$ ,  $\delta = 0.05$ ,  $\rho_u = 1$ ,  $\rho_d = 0, 0.9$ ,  $O_2 = 3$ , and  $W = 85, 90, 95$ ; recall the obstacle is placed in the middle of the strip. The main features are: the presence of a jump across the obstacle and the dependence of the profile on the horizontal coordinate.

A deeper insight in the structure of the density profile can be reached by looking at the horizontally averaged densities.

Figures 4.7 and 4.8 show the profile  $\tilde{\rho}(x)$  for different values of the parameters  $W = 0, 10, \dots, 90, 95$ ,  $\delta = 0.1$  and  $\delta = 0.01$ , and bottom boundary density  $\rho_d = 0, 0.4, 0.5, 0.6, 0.7, 0.8, 0.9$ . The remaining parameters are not changed and are listed in the captions.

Here we see the drastic change in the density profile behavior when the drift value decreases from 0.1 to 0.01. When  $\delta > 0.1$  and  $W = 0$ , the density profile is nearly independent of  $x$  and is equal to 0.5. It will not vary with  $\rho_d$ , as long as  $\rho_d < 0.5$ . When  $\rho_d > 0.5$ , the average value of the density increases with  $\rho_d$  and is equal to it. The case  $\delta = 0.01$  is reminiscent of the zero drift behavior, whereas the case  $\delta = 0.1$  is qualitatively different.

We focus, now, in this latter case  $\delta = 0.1$ . Each panel in Figures 4.7 and 4.8 refers to a fixed value of the bottom boundary density  $\rho_d$  and the different curves refer to different values of the obstacle width  $W$ . In each a panel a quite obvious behavior is observed: the jump in stationary density measured at the obstacle increases with its width.

Much more interesting is the dependence of the density profile on the bottom boundary density at fixed obstacle width. Consider, for example, the case  $W = 50$  which corresponds to the black lines in Figures 4.7 and 4.8. The curve depicted in the top left panel in Figure 4.7 refers to the case  $\rho_d = 0$ : in the upper part of the strip (above the obstacle) the density profile is essentially constant and drops to 0.73 at the obstacle. Immediately below the obstacle the density falls to 0.25, stays approximately constant for the whole bottom part of the strip, and finally drops to zero to match the boundary condition.

This behavior does not change that much when  $\rho_d$  is

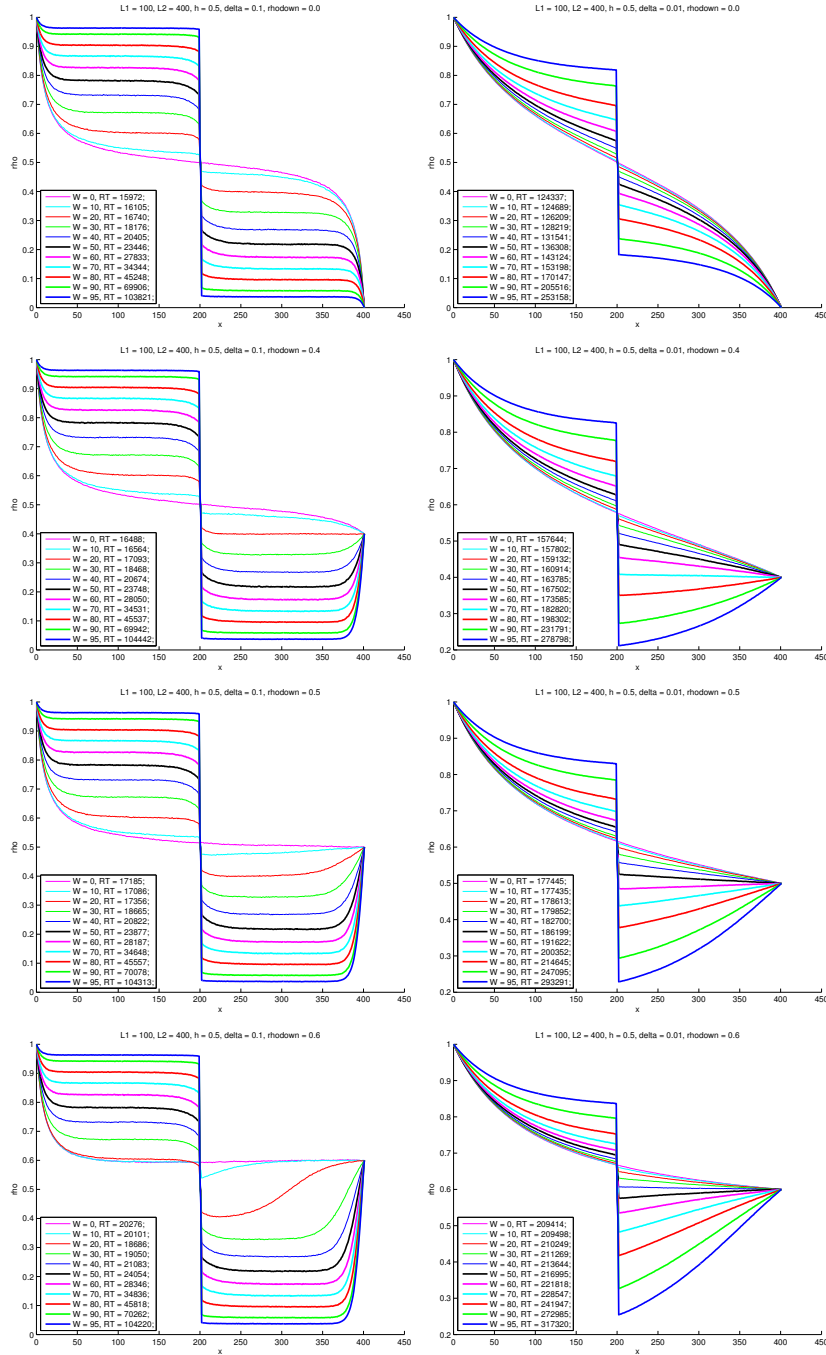


FIG. 4.7. Density profile obtained by averaging the 2D lattice simulation: comparison for different  $W$ . The lattice size is  $100 \times 400$ ,  $h = 0.5$ ,  $\delta = 0.1$  (left) and  $\delta = 0.01$  (right),  $\rho_u = 1$ ,  $\rho_d = 0, 0.4, 0.5, 0.6$  from the top to the bottom, and  $O_2 = 3$ . The residence time measured in the different cases has been reported in the inset.

increased till  $\rho_d = 0.7$ : the density profile lays, indeed, on the reference skeleton provided by the  $\rho_d = 0$  case differing from it only in the final part where the different boundary condition must be matched. The picture is completely different when  $\rho_d$  gets larger than the critical value 0.73: in the upper part of the strip the density pro-

file is approximately constant and equal to the bottom boundary condition, whereas in bottom part it departs from the reference skeleton and immediately below the obstacle it starts increasing to match the boundary condition.

This description is qualitatively analogous for any

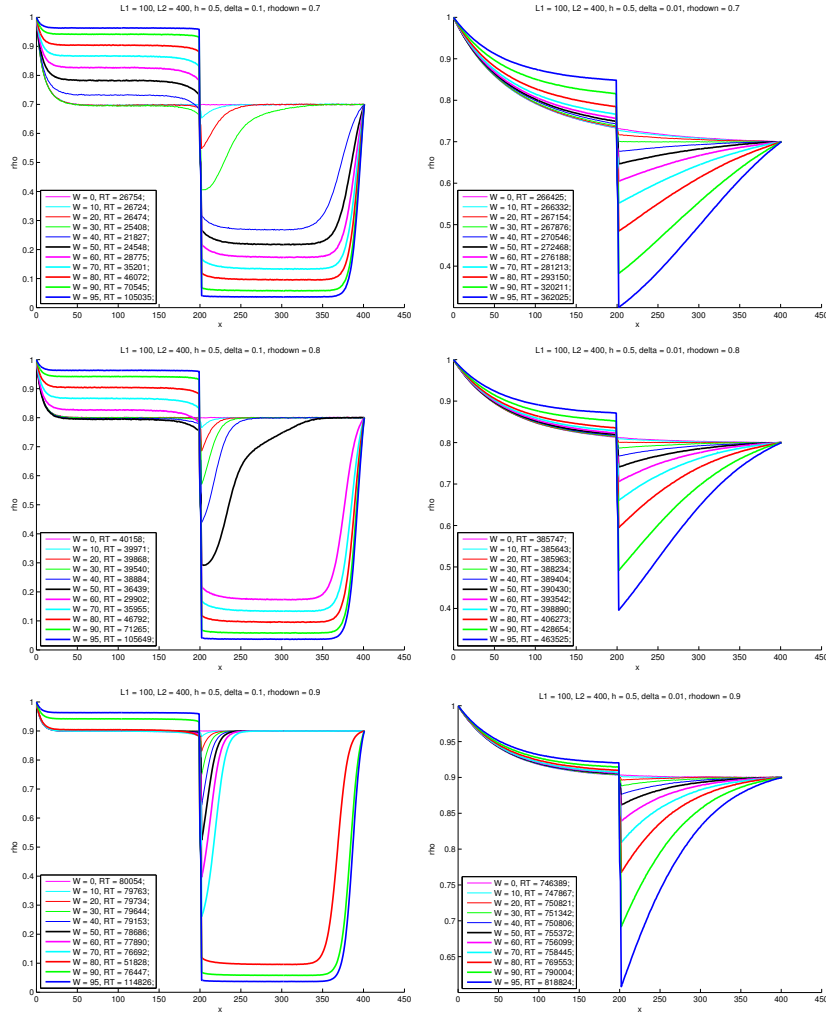


FIG. 4.8. The same as in Figure 4.7 excepted for the bottom boundary density:  $\rho_d = 0.7, 0.8, 0.9$  from the top to the bottom.

value of the obstacle width  $W$ . Obviously the value of the critical density measured on the upper face of the obstacle in correspondence of the skeleton profile obtained for  $\rho_d = 0$  changes with  $W$ , but it is interesting to remark that it tends to 0.5 (the value measure in absence of the obstacle) as the width of the obstacle is decreased.

Summarizing, there exist two different regimes (controlled by  $\rho_d$ ) for  $\delta > 0$  of the obstacle, no onset of percolation. When  $\rho_d > 0.5$ , depending on the obstacle width, the system can be in the low flux regime with onset of percolation.

This behavior is very similar to the phase transition which is observed in the 1D simple exclusion model [10] with critical bottom boundary density 0.5 (see, also, [1] for the the obstacle free strip geometry [1]). Here, the critical bottom density is not 0.5 but it is given by the density on the obstacle measured in the reference skeleton

profile corresponding to  $\rho_d = 0$ . From the physical point of view the two phases differ for the particle content in the bottom part of the strip: such a region is almost empty in one case and pretty full in the other. This behavior of the density profile has obviously an important effect on the residence time.

As we have already remarked above, this qualitative change in the density profile is not observed in the zero drift case. Such a peculiar behavior that, as we shall see in the following, has also a relevant consequence on residence times, is due to the combined effects of the obstacle and the external drift.

## B. Residence time

In all the cases discussed Section IV A we have computed the residence time and reported it in the inset in

$W$	$R_{LA}$	$R_{MF}$	$m_1$	$m_2$	$R_{LA}$	$R_{MF}$	$m_1$	$m_2$
0	15972	16165	80.5	200.9	124110	127267	633	201.1
10	16105	16215	80.7	200.9	124526	126405	629	200.9
20	16740	16577	82.5	201.0	125953	125501	624	201.0
30	18176	18476	92.0	201.0	128020	129696	645	201.0
40	20405	20906	104.0	200.9	131285	128462	639	201.0
50	23445	24252	120.6	201.0	135984	132939	662	200.9
60	27833	27914	138.9	201.0	142879	140895	701	201.0
70	34344	35402	176.1	201.0	152902	148000	736	201.1
80	45248	46583	231.8	201.0	169800	174161	866	201.2
90	69905	76254	379.4	201.0	205000	212743	1058	201.0
95	103821	120039	597.3	201.0	252167	267808	1332	201.1

TABLE I. Comparison between the residence time of the lattice simulation with  $\rho_d = 0.0$  and its Mean Field approximation, based on the averaged simulated density profile, along with its components. The quantities  $m_1$  and  $m_2$  are defined in equation (4.16). The other parameters are as in Figure 4.7, in particular  $\delta = 0.1$  is on the left and  $\delta = 0.01$  is on the right.

Figures 4.7 and 4.8. For convenience we summarize the data corresponding to  $\rho_d = 0, 0.9$  in Tables I and II together with the Mean Field estimate (1.5) computed by using the horizontally averaged density profile  $\bar{\rho}(x)$ . We remark that in this case this procedure will not give an accurate prediction for the residence time due to the lacking of horizontal translational invariance in the density profile, nevertheless, as the data will show, the prediction will be at least qualitatively sound. Moreover, on the basis of the Mean Field approximation it will be possible to interpret the Monte Carlo results.

In view of our results on the structure of the density profile we know that, for  $\delta > 0$ , there exists two different regimes controlled by  $\rho_d$ . The difference in the residence time behavior is illustrated by Figure 4.9 that shows the residence time as a function of  $\rho_d$ . Indeed, for  $\rho_d < 0.5$  there is only a weak dependence on  $\rho_d$ , whatever is the obstacle with  $W$ . For  $\rho_d > 0.5$ , depending on  $W$ , there is a large increase of residence time with  $\rho_d$  itself. A simple interpretation of this fact is the following: when the bottom boundary density is large the system is in the low flux regime and bottom part of the strip is so highly populated that the residence time becomes large. But, as we shall see in the following, a deeper understanding of this phenomenon can be achieved by means of the Mean Field approximation.

Recall the Mean Field approximation (1.5) of the residence time and note that  $R$  is written as a product of

$W$	$R_{LA}$	$R_{MF}$	$m_1$	$m_2$	$R_{LA}$	$R_{MF}$	$m_1$	$m_2$
0	80054	80953	223.3	362.5	735757	803550	2186	367.6
10	79763	80066	221.0	362.2	737664	795020	2163	367.6
20	79734	82502	228.0	361.9	738747	810731	2207	367.4
30	79644	81053	224.5	361.1	739715	806241	2197	366.9
40	79153	81185	225.7	359.7	739925	812013	2217	366.3
50	78686	79679	222.8	357.7	743705	812770	2223	365.5
60	77890	79146	223.2	354.6	744789	831905	2283	364.4
70	76692	78093	223.4	349.5	746229	846801	2334	362.7
80	51828	54286	237.7	228.4	755008	858597	2382	360.5
90	76447	80147	369.3	217.0	773265	874445	2455	356.1
95	114826	120569	560.6	215.1	801341	877180	2501	350.8

TABLE II. Comparison between the residence time of the lattice simulation with  $\rho_d = 0.9$  and its Mean Field approximation, based on the averaged simulated density profile, along with its components. The quantities  $m_1$  and  $m_2$  are defined in equation (4.16). The other parameters are as in Figure 4.7, in particular  $\delta = 0.1$  is on the left and  $\delta = 0.01$  is on the right.

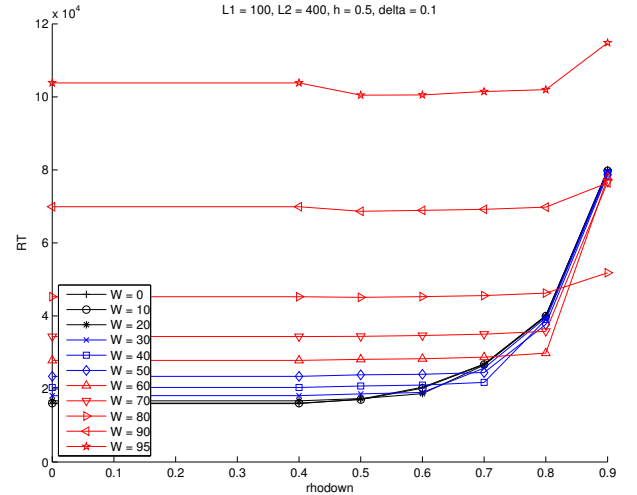


FIG. 4.9. Residence time as a function of  $\rho_d$  for the different values of  $W$  listed in the inset. Parameters:  $L_1 = 100$ ,  $L_2 = 400$ ,  $h = 0.5$ ,  $\delta = 0.1$ ,  $\rho_u = 1$ , and  $O_2 = 3$ .

two terms: the area under the density profile and a factor depending on the slope of the density profile at the top boundary. Hence, it is convenient to introduce the quantities

$$m_1 = -\frac{2}{(1-h)\rho'(0)} \quad \text{and} \quad m_2 = \int_0^{L_2} \rho \quad (4.16)$$

and write  $R = m_1 m_2$ . The values of  $m_1$  and  $m_2$  for the simulations discussed in this section are listed in Tables I and II.

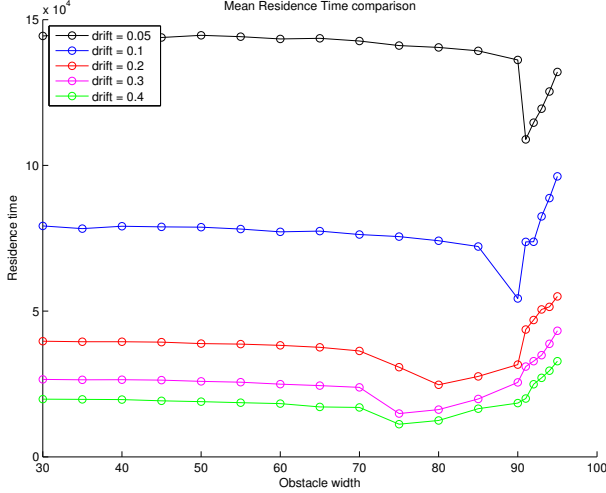


FIG. 4.10. Residence time as a function of the obstacle width  $W$  for the different values of  $\delta$  listed in the inset. Parameters:  $L_1 = 100$ ,  $L_2 = 400$ ,  $h = 0.5$ ,  $\rho_u = 1$ ,  $\rho_d = 0.9$ , and  $O_2 = 3$ .

A deeper insight in the problem is possible by looking at the dependence of the residence time on  $W$ . We distinguish the two regimes discussed above.

*Regime  $\rho_d < 0.5$ .* We note that the residence time increases uniformly with increasing  $W$  as seen in Figure 4.9. Note also that the behavior of the residence time does not depend on the value  $\rho_d$ ; we can then focus on the case  $\rho_d = 0$ . In terms of the Mean Field approximation this is due to the variation of the derivative of the profile at the top boundary. Indeed, see the values listed in the left part of Table I, the parameter  $m_2$  stays constant, whereas  $m_1$  steadily increases with the obstacle width. This is due to an increased density before the barrier that changes the slope  $\rho'(0)$ . On the other hand, the increase in density before the barrier and the developing wake behind the barrier cancel and this explains why  $m_2$  stays constant.

*Regime  $\rho_d > 0.5$ .* As long as the drift is small (check the right value in the Tables I-II), the dependence of residence time on  $W$  is similar to the case when the drift is zero. The dependence on  $W$  is dominated by the diffusion and the residence time increases with increasing  $W$ , similar to the no drift case.

When  $\delta$  is large, that is to say it exceeds a particular value compared to the diffusion constant, a new dependence of the residence time on  $W$  appears, see the data in the left in Table II and Figure 4.10. Now there is an initial decrease in the residence time with increasing  $W$  until a critical value of  $W_c$  is reached where there's a dip in residence time. This critical width depends on the pa-

rameters of the model: from the full set of data listed in the insets in Figures 4.7 and 4.8 it is possible to extract  $W_c$  for all the considered values of  $\rho_d$  and observe that the ratio between the critical width  $W_c$  and  $L_1$  becomes close in value to  $\rho_d$  when  $\rho_d$  is high. Moreover,  $W_c$  decreases with drift and the width of the dip around  $W_c$  increases with drift.

This phenomenon is observed for any value of  $\rho_d$  larger than 0.5, but the larger is  $\rho_d$  the more evident the phenomenon is. We focus on the case  $\rho_d = 0.9$  and  $\delta = 0.1$ . From the plots in the corresponding panel on the left in Figure 4.8 we see that, when  $W$  is increased from 0 to 70, the density profile in the upper part of the strip remains essentially unchanged, whereas a wake below the barrier appears. The appearance of such a wake decreases the value of  $m_2$  and hence the residence time. Physically, it means the number of particles in the bottom part of the strip decreases and, thus, the typical time to cross such a region gets lower. This is confirmed by the data on the left in Table II: the decrease of  $m_2$  from 362.5 to 349.5 causes the reduction of the residence time from 80054 to 75592.

If  $W$  is further increased, the coefficient  $m_2$  goes on decreasing, but the residence time increases due to jamming. This is quantified from derivative and density integrals. The system is in the fast flux regime, so that the density increase in front of the barrier determines the increase. This is illustrated in Table II, indeed, the coefficient  $m_1$ , which is essentially constant for  $W = 0, 10, \dots, 70$ , starts to increase when  $W$  exceeds 80.

We observe that initially there is no change in the density before the barrier (specifically in  $\rho'(0)$ ), but a wake develops. The initial decrease in the residence time is therefore due to the decreased density of the wake. This dependence on  $W$  is very different from the one observed in the previous cases, where there is always a substantial increase in density before the barrier. The difference must relate to the onset of percolation, so that a decrease in the wake density has a large effect. The distance dependence of the density profile in the wake changes from convex to concave beyond  $W_c$ . The minimum in  $W_c$  occurs when the wake density reaches its minimum. Then there is no further reduction in the density possible and the density before the barrier now increases steeply with increasing  $W$ . The increase in residence time with  $\rho_d$  as well as the distribution before the barrier is now very similar to the other regime, that also suggests the importance of increased percolation, that results in jamming

type behavior.

## V. DISCUSSION AND CONCLUSIONS

According to the lattice model simulations reported in this paper, the effect of the barrier on the residence time is surprising: at low flux the system may show decreased residence time of particles when passage barrier is increased, instead of the expected decrease in residence time.

We find three different flow regimes of interest. The regime of zero drift, where the residence time increases with barrier length. The barrier generates an increase in density before the barrier and a wake behind. The density changes are comparable. The increase in residence time is due to the lowered derivative of density at the entrance of the stripe, that is due to the increased density before the barrier. The concentration of particles before the barrier is such that these particles can be considered to be in the percolation regime. The system becomes increasingly jammed.

The regime of non-zero drift, but with an exit density  $\rho_d < 0.5$ . This is the regime of high flux (see [1, 10, 17]) without percolation inhibition. The residence time in this regime is independent of the bottom boundary density. When the barrier increases the residence time increases for a similar reason as in the zero-drift case. When  $W/L_1$  becomes larger than 0.5 the residence time increases steeply and the density before the barrier increases such that it is in the percolation regime. It is dominated again by the derivative of density at the entrance of strip.

The regime of non-zero drift, but with exit density  $\rho_d > 0.5$ . This is the regime of low flux. When the Damköhler number, i.e., the ratio between the external drift and the diffusion coefficient, is sufficiently large, the non-linear dependence of residence time on the barrier width appears. The residence time decreases with increasing value of barrier  $W$  until a limiting value of  $W_c$  is reached. This critical width is such that its ratio with the horizontal length of the strip is equal or less than  $\rho_d$ . Beyond this value of  $W$  the residence time increases steeply with increasing  $W$ , as expected for the onset of increased jamming.

The difference between the high flux and low flux regime is due to the very different dependence of  $\rho(x)[1 - \rho(x)]$  when  $x \in [0, L_2]$ . More precisely, consider the  $\rho(x)$  plots in Figures 4.7 and 4.8, the related graphs of the

function  $\rho(x)[1 - \rho(x)]$  behave as follows: as long as  $\rho_d < 0.5$  the function  $\rho(x)[1 - \rho(x)]$  will have a maximum in  $x \in [0, L]$ , since  $\rho$  varies between  $\rho_d \leq 0.5$  and 1.

The derivative of  $\rho(x)[1 - \rho(x)]$  varies from negative to positive when  $\rho'(x) > 0$  or the opposite way when  $\rho'(x) \leq 0$ . When  $\rho_d > 0.5$  the sign of the derivative of  $\rho(x)[1 - \rho(x)]$  depends on  $\rho'(x)$ . It is always positive ( $\rho'(x) < 0$ ) or negative ( $\rho'(x) > 0$ ). The contribution of drift to current is proportional to the  $x$  derivative of  $\rho(x)[1 - \rho(x)]$ . Since this can only become zero, when  $\rho_d < 0.5$  or  $\rho'(x) = 0$ , the zero drift and drift curves only cross when  $\rho_d < 0.5$ . This causes the density distribution when drift is not zero to be less than that of the drift zero density distribution. It becomes equal to  $\rho_d$  over a large density regime when  $\rho_d > 0.5$  and drift exceeds a particular value (this value falls between 0.1 and 0.01 in Figures 4.9 and 4.10).

The changes in residence time in presence of barrier can be understood as maximization of current.

In Figure 4.11 the changes in density for  $\rho_d < 0.5$  and  $\rho_d > 0.5$  are schematically sketched. There is an important qualitative difference between the two cases.

The case  $\rho_d < 0.5$  (Figure 4.11 first and second panel from the left): the barrier reduces transmission from  $x < L_2/2$  to  $x > L_2/2$ , since the density gradient at  $x = L_2/2$  has the same sign before and after barrier. Also directly behind the barrier  $\rho'(x) < 0$ , since this gives a positive contribution to the flow rate, the density dependence on  $x$  then is concave. Reduced transmission through the barrier increases the density before the barrier into the  $\rho_d > 0.5$  regime, that is the percolation regime. Behind the barrier a wake develops of lower density. The flow rates before as well after the barrier decrease.

The case  $\rho_d > 0.5$  (Figure 4.11 third and fourth panel from the left): when  $\rho_d > 0.5$  the  $x$  derivative of  $\rho(x)[1 - \rho(x)]$  is negative as long as  $\rho'(x) > 0$ . An initial convex shape of density profile of the wake behind the barrier implies  $\rho'(x) > 0$  ( $x > L_2/2$ ). The flow rate now increases, because in the wake the density is reduced and  $\rho(x)[1 - \rho(x)]$  then increases. Density reduction when barrier width is small is initially in the percolation regime. Since the derivative  $\rho'(x)$  before the barrier is negative and positive after the barrier, the second derivative of  $\rho(x)$  is discontinuous. Barrier transmission is not hindered as long as  $W < W_c$ , where the derivative  $\rho'(x)$  changes sign. When  $W$  remains less than  $W_c$  there is no increase in density before the barrier. At

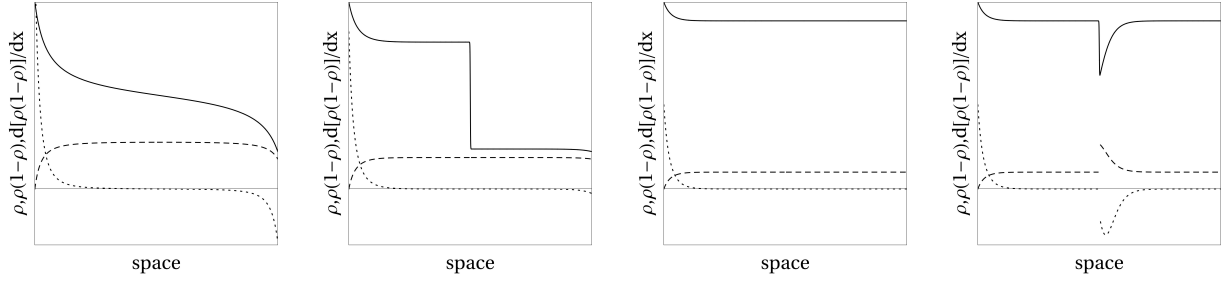


FIG. 4.11. Schematic (qualitative) representation of the density profiles (solid lines) in the absence and presence of barrier of small width and with not zero drift. No quantitative information is provided in the picture except for the zero which is represented by the thin solid horizontal line. From the left to the right:  $\rho_d < 0.5$  and no barrier,  $\rho_d < 0.5$  with barrier at  $L_1/2$ ,  $\rho_d > 0.5$  and no barrier,  $\rho_d > 0.5$  with barrier at  $L_1/2$ . Dashed lines represent  $\rho(x)[1 - \rho(x)]$  and dotted lines represent its derivative  $d\{\rho(x)[1 - \rho(x)]\}/dx$ .

this condition the fast flow in the wake of barrier drains density from the front of the barrier, so that it is maintained at the density it also has in absence of the barrier. The current increases with increasing barrier width, until no density reduction in the wake is any more possible and the initial sign of  $\rho'(x)$  becomes negative. Then reduced transmission through the barrier increases density before the barrier and current decreases.

This analysis has been done for the projection of the two dimensional changes in density onto a one dimensional density. In the two dimensional case, a relative value of the horizontal displacement  $h = 0.5$  has been used. In that case there is rapid diffusion of density before the barrier to the opening positions between barrier and wall, and after the barrier into the wake region. In the low flux region, the low density that develops in the wake also reduces density between barrier and wall so that density transport from before the barrier to the open space region is enhanced. The one dimensional analysis

indicates that asymmetrical density development is indeed caused by the convex residence time function of  $\rho$  in the high flux region, that ultimately is due to percolation.

In the recent paper [19] the totally asymmetric simple exclusion process has been applied to a molecular motor transport model on a network. Whereas the network is different from our strip model and drift equals one, the paper [19] finds also non-linear dependence on motor particle density when its global density exceeds a critical value and network exit rate is asymmetric. Also in this case the critical behavior depends on the derivative of  $\rho(x)[1 - \rho(x)]$  as we propose in this paper.

#### ACKNOWLEDGMENTS

ENMC acknowledges ICMS (TU/e) for the kind hospitality and financial support. OK acknowledges support from the “Over Grenzen, complexiteit programma” of KNAW (Royal Netherlands Academy of Sciences and Arts).

- 
- [1] E.N.M. Cirillo, O. Krehel, A. Muntean, R. van Santen, A. Sengar, “Residence time estimates for asymmetric simple exclusion dynamics on strips.” *Physica A* **442**, 436–457 (2015).
  - [2] A. Ahrony, D. Stauffer, “Introduction to Percolation Theory.” Taylor and Francis, 1994.
  - [3] J. Sane, J. T. Padding, A. A. Louis, “Taylor dispersion of colloidal particles in narrow channels.” *Molecular Physics* **113**, 2536–2545 (2015).
  - [4] A. Schadschneider, D. Chowdhury, K. Nishinari, “Stochastic Transport in Complex Systems: From Molecules to Vehicles”, Elsevier, 2010.
  - [5] D. Braess, “Über ein Paradoxon der Verkehrsplanung.” *Unternehmensforschung* **12**, 258–268 (1968).
  - [6] A. Garcimartin, J.M. Pastor, L.M. Ferrer, J.J. Ramos, C. Martin-Gomez, I. Zuriguel, “Flow and clogging of a sheep herd passing through a bottleneck.” *Physical Review E* **91**, 022808 (2015).
  - [7] I. Zuriguel, D.R. Parisi, R.C. Hidalgo, C. Lozano, A. Janda, P. A. Gago, J. P. Peralta, L. M. Ferrer, L. A. Pugnaloni, E. Clement, D. Maza, I. Pagonabarraga, A. Garcimartin, “Clogging transition of many-particle systems flowing through bottlenecks.” *Scientific Reports* **4**, 7324 (2014).

- [8] D. Helbing, L. Buzna, A. Johansson, T. Werner, “Self-organized pedestrian crowd dynamics: Experiments, simulations, and design solutions.” *Transportation Science* **39**, 1+24 (2005).
- [9] K. Suzuno, A. Tomoeda, M. Iwamoto, D. Ueyama, “Dynamic structure in pedestrian evacuation : Image processing approach.” *Traffic and Granular Flow* **39**, eds. M. Chraïbi, M. Boltes, A. Schadschneider, A. Seyfrid (2013).
- [10] J. Krug, “Boundary-induced phase transition in driven diffusive systems.” *Physical Review Letters* **67**, 1882–1885 (1991).
- [11] M. J. Simson, K. A. Landman, B. D. Hughes, “Multi-species simple exclusion processes.” *Physica A* **388**, 399–406 (2015).
- [12] J. Bear, “Dynamics of Fluids in Porous Media”, Dover, 1972.
- [13] E.N.M. Cirillo, A. Muntean, “Can cooperation slow down emergency evacuations?” *Comptes Rendus Mécanique* **340**, 6260–628 (2012).
- [14] E.N.M. Cirillo, A. Muntean, “Dynamics of pedestrians in regions with no visibility – a lattice model without exclusion.” *Physica A* **392**, 3578–3588 (2013).
- [15] D. Andreucci, D. Bellaveglia, E.N.M. Cirillo, S. Marconi, “Monte Carlo study of gating and selection in Potassium channels.” *Physical Review E* **84**, 021920 (2011).
- [16] N.G. van Kampen, “Stochastic Processes in Physics and Chemistry.” Elsevier Science, 1981.
- [17] M.R. Evans, N. Rajewsky, E.R. Speer, “Exact solution of a cellular automaton for traffic.” *Journal of Statistical Physics* **95**, 45–96 (1999).
- [18] P. Bastian, M. Blatt, A. Dedner, C. Engwer, R. Klöfkorn, R. Kornhuber, M. Ohlberger, O. Sander, “A generic grid interface for parallel and adaptive scientific computing. Part II: Implementation and tests in DUNE.” *Computing* **82**, 121–138 (2008).
- [19] D.V. Denisov, D.M. Miedema, B. Nienhuis, P. Schall, *Phys. Rev. E* **92**, 052714 (2015).